Suppressing Dissipative Paths in Superconducting Coplanar Waveguide Resonators

J. M. Hornibrook, E. E. Mitchell, and D. J. Reilly

***Abstract*—The electromagnetic environment can have a significant effect on the resonant line-shape and loaded Q-factor of superconducting coplanar waveguides in the low temperature (< 100 mK) and low microwave power regime. Here, electromagnetic simulations are used to visualize the electric field strength throughout the resonator environment, highlighting situations in which parasitic modes lead to increased dissipation. Methods used to suppress parasitic coupling include increasing the density of wire bonds and vias, reducing the width of the transmission line (whilst maintaining the characteristic impedance at 50 Ω) and establishing strong grounding to the sample enclosure. The effect of reducing the parasitic coupling on the microwave transmission spectrum is reported.**

***Index Terms*—Microwave coplanar waveguide, superconducting, two-level systems.**

I. Introduction

SUPERCONDUCTING coplanar waveguide (CPW) resonators with high quality $(Q-)$ factors are used in single photon detection [1], parametric amplification [2], and coherent coupling to quantum two-level systems [3]. Intrinsic resonator losses have been studied extensively, particularly in the low power regime, whereby cavity photons couple to two-level systems associated with defects in the dielectric or at the interface between substrate and resonator [4], [5]. Here we discuss a loss mechanism that originates from parasitic dissipation in the environment external to the resonator. Although not intrinsic to the resonator, this parasitic pathway leads to an unwanted loading of the resonator and suppression of Q-factor, even in the regime where entry and exit ports have been designed to be under-coupled. An asymmetry in the line-shape of the resonance provides a signature that parallel parasitic pathways are present.

We report measurements of the microwave response of niobium superconducting resonators, elucidating the effect of this parasitic dissipation. Taken together with electromagnetic simulations, we suggest methods to suppress this artificial loss mechanism.

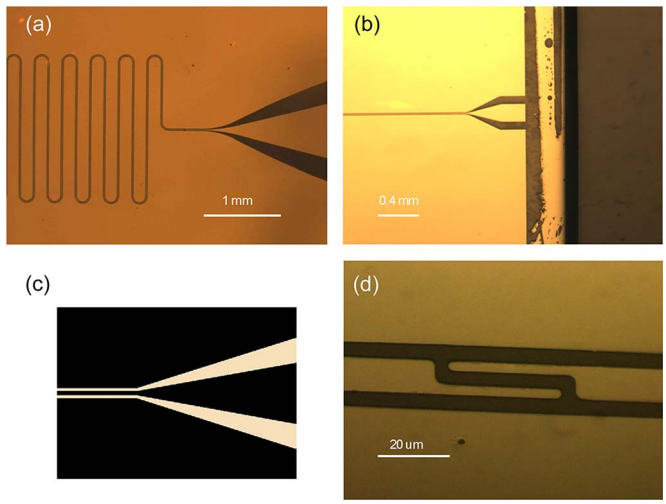

Fig. 1. Nb CPW resonator showing (a) large and (b) small contact pad arrangement. (c) Schematic of an abruptly tapered contact pad. (d) 2.0 fF gap capacitor located either end of the resonator.

II. Experimental Methods

Nb half-wavelength CPW resonators were fabricated on sapphire and magnesium dioxide (MgO) substrates of size 10 mm × 5 mm. The substrate surfaces were cleaned using ion beam milling (300 V) before an *in-situ* 150 nm film was sputtered at 5×10^{-7} mb, yielding current densities of $J_c \sim 14$ MAcm^{-2}. The CPW was patterned using optical lithography with excess metal removed via argon ion beam milling. The center track of the coplanar waveguide is 10 μm wide with insulating gaps 4.6 μm designed to give a characteristic impedance of 50 Ω on both r-cut sapphire and MgO. Two different contact pad geometries are shown in Fig. 1(a) and (b). The resonator is connected to highly attenuated (60 dB) and filtered input and output ports via inline capacitors that ensure the resonator is in the under-coupled regime [Fig. 1(d)] [6]. Resonator lengths are ∼15 mm, with adjacent loops separated by 180 μm to prevent electromagnetic coupling [Fig. 1(a)]. These lead to resonances in the range $f_0 \sim 3-5$ GHz.

The chip is positioned in a recessed slot and wire bonded to a printed circuit board (PCB) using 25 μm diameter Al wire bonds closely spaced with three wire bonds at each center conductor and around 100 wire bonds around the perimeter of the chip (see Section III-B) to ensure strong grounding between the Nb resonator ground plane and sample box. The PCB (Rogers laminate RO6010) is a ceramic-filled PTFE laminate used to

Manuscript received October 10, 2012; accepted February 19, 2013. Date of publication March 7, 2013; date of current version April 3, 2013. This work was supported by the Australian Research Council Centre of Excellence Scheme (EQuS CE110001013).

J. M. Hornibrook is with the CSIRO Materials Science & Engineering, Lindfield, 2070 NSW, Australia. He is also with the School of Physics, University of Sydney, Sydney, NSW 2006, Australia (e-mail: john.hornibrook@csiro.au).

E. E. Mitchell is with the CSIRO Materials Science & Engineering, Lindfield, 2070 NSW, Australia (e-mail: emma.mitchell@csiro.au).

D. J. Reilly is with the ARC Centre of Excellence for Engineered Quantum Systems, School of Physics, University of Sydney, Sydney, NSW 2006, Australia (e-mail: reilly@physics.usyd.edu.au).

Color versions of one or more of the figures in this paper are available online at http://ieeexplore.ieee.org.

Digital Object Identifier 10.1109/TASC.2013.2251055

closely match the dielectric constant to the substrates (MgO: 9.5; sapphire: 9.4; Rogers 6010: 10.2), with 35 μm Cu and a thin layer of wire bondable gold on the top surface, whose base is soldered into a light-tight copper sample enclosure. The PCB features a coplanar waveguide with a tapered center conductor to match the SMA connector geometry (Super SMA, Southwest Microwaves) to the contact pads on the resonator chip. Multiple vias connect ground planes on the top and bottom of the PCB in order to prevent direct parasitic EM coupling between input and output ports via slot-line modes.

The enclosure is mounted on the mixing chamber of a dilution refrigerator. Resonator losses were determined via S-parameter measurements using a microwave vector network analyzer (VNA, N5230C Agilent Co, 8510C HP Co) together with room temperature and cryogenic amplification (Low Noise Factory, +42 dB gain).

III. Electromagnetic Simulations

The resonator, PCB, and sample box were simulated using a finite element 3D EM field solver (Ansoft HFSS 14). The simulations show that appreciable power can couple from input to output ports via pathways that are parallel to the resonator, for instance, via currents that flow along the surface of the PCB. Interference of these parallel signals with those that are transmitted directly through the resonator can contribute to the asymmetry in the resonator line-shape. We note that because of this interference, dissipation in the parallel pathway can effectively load the resonator beyond the limit set by the coupling capacitors and strongly reduce the loaded Q-factor.

From our EM simulations it was determined that the following aspects contribute to the strength of this parallel, parasitic pathway: (1) the number of Al wire bonds connecting the ground plane of the CPW to the ground plane of the PCB, (2) the number of vias, (3) the width of the waveguide and microwave launcher at the SMA connector, (4) the geometry of the tapering of the contact pads [7], (5) the matching of the launching pin diameter (150 μm) of the SMA connectors to the width of the PCB contact pad and (6) the length of the launching pin (to suppress direct radiative coupling). Below we discuss these aspects in detail in an effort to suppress this parasitic pathway that artificially loads the resonator.

A. Low Parasitic Environment

Well-connected ground planes with extensive vias and wire bonds reduce the parasitic current density in addition to preventing resonant modes in the dielectric. Fig. 2(a) compares simulation results overlaid with an image of the outer copper sample box and SMA connectors (grey) with launching pins connected to the CPW of the PCB containing an array of vias (small circles). The small rectangle in the center represents the sample chip. Small lines all the way around the chip denote wirebonds connecting the chip to the PCB. A large amount of solder around the edges of the PCB is used to ground the PCB to the sample box. In the optimized design [Fig. 2(a)] there are wirebonds spaced every 320 μm. The via spacing was 1.7 mm, with radius 180 μm. These simulations illustrate the extent to which such technical considerations can control the magnitude of the E-field off-chip and well away from the coplanar structure that defines the resonator. As we have discussed, dissipation in these parallel channels loads the resonator, even when the coupling capacitors are chosen to ensure the resonator is under-coupled.

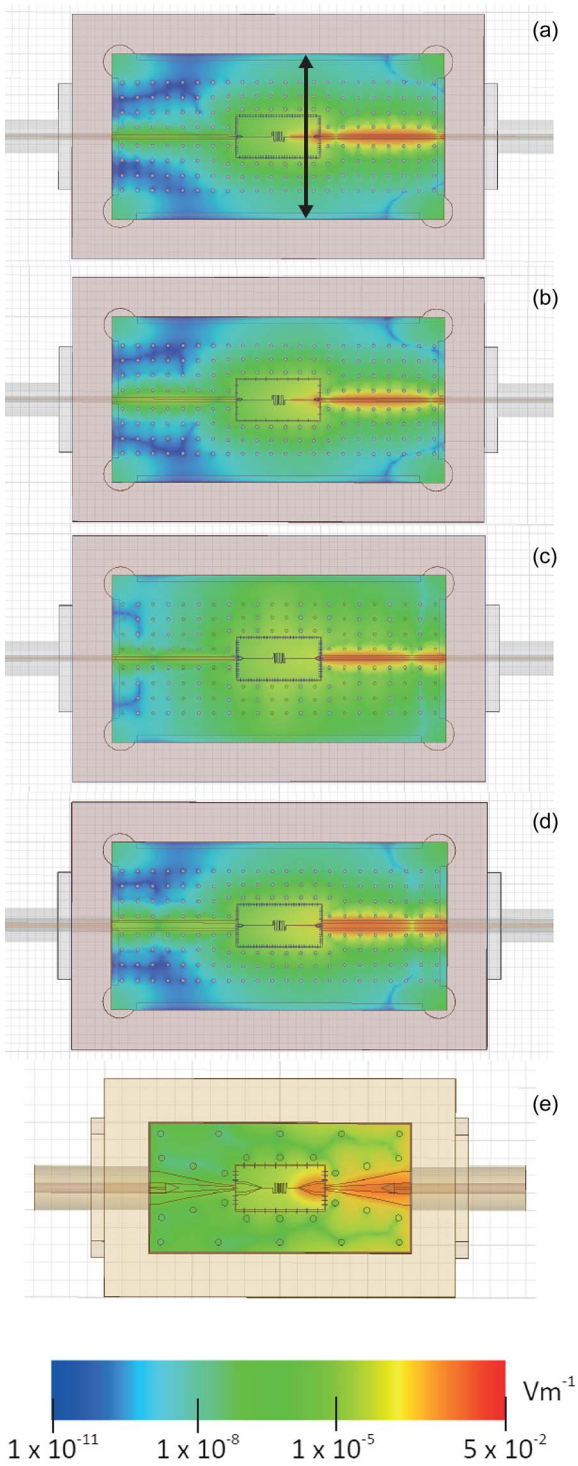

Fig. 2. Simulations of the parasitic electric field magnitude 250 μm below the CPW plane in the PCB dielectric using Ansoft's HFSS at -90 dBm input powers near the resonant frequency f_o, for a CPW with (a) the parasitic field minimized (b) using 1/3 of the wire bonding used in Fig. 2(a) and (c) doubling the via spacing. (d) Effect of increasing the center conductor width. (e) Combined effects of low-density wirebonds and vias, wide central tracks together with large tapered contact pads.

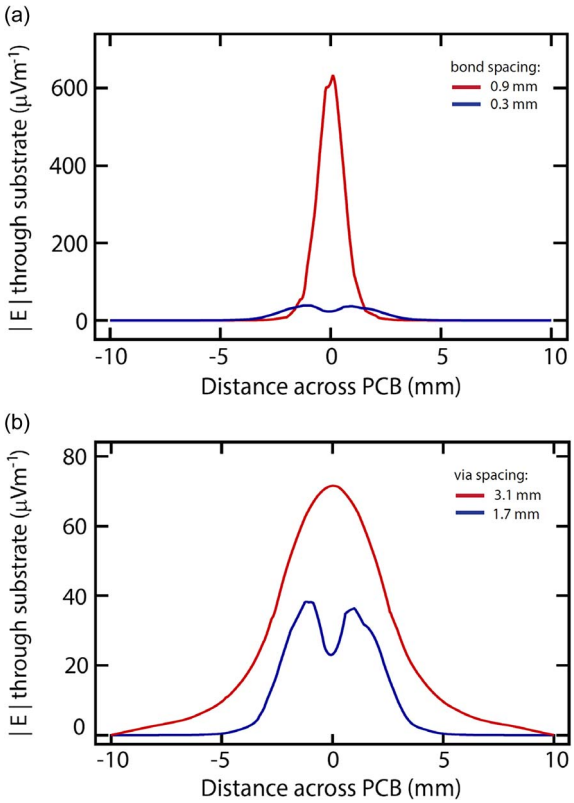

Fig. 3. Simulations of the E-field strength across the sample box (short side) just below the CPW resonator with (a) wirebonds spaced every 300 μm (blue) compared with every two out of three wires bonds removed (red) and (b) the via spacing increased from 1.7 mm (blue) to 3.1 mm (red).

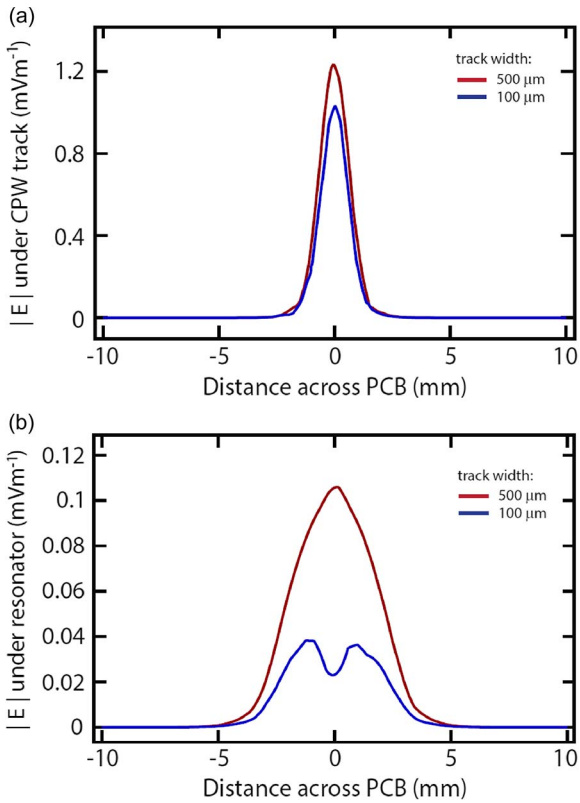

Fig. 4. Simulations of the E-field strength across the sample box (short side) for a CPW with a 100 μm wide (blue) and 500 μm (red) PCB center conductor width whilst maintaining 50 Ω characteristic impedance. The plots are given for (a) 250 μm below the PCB top surface and (b) just below the CPW resonator.

B. Increasing Wire Bonding and Via Density

In Fig. 2(b), we plot the simulated magnitude of the electric field at a frequency close to resonance on a sheet 250 μm below the top metal layers when the wire bond spacing has been increased to 0.9 mm (a 66% reduction in wirebonds). The advantage of close wire-bonding is further demonstrated in Fig. 3(a) by comparing the E-field on a linear scale directly under the CPW resonator, in a line perpendicular to the CPW direction [black line, Fig. 2(a)]. The E-field increases by a factor of 12 when two thirds of the wire bonds are removed.

Likewise, when the via spacing is increased from 1.7 mm to 3.1 mm [Fig. 2(c)], the overall E-field increases throughout the PCB (extended green and yellow regions $\sim$10 μVm^{-1} range) compared with the simulation in Fig. 2(a). Doubling the via spacing increases the E-field by 1.8 times under the center conductor, with the remnant field strength remaining at 10 μVm^{-1} up to 5 mm from the center conductor [Fig. (3b)]. A reduction in stray fields was observed when the via spacing was reduced below $\lambda/20$.

C. CPW Width

By minimizing the width of the CPW on the PCB, especially near the SMA launching pin, direct radiative coupling can be reduced. We illustrate this kind of coupling in Fig. 2(d), by increasing the width of the CPW central conductor by a factor of 5 (to 500 μm) in the simulations. In this instance the E-field strays much further from the CPW [red area in Fig. 2(d)] and is higher in magnitude throughout the PCB compared with Fig. 2(a). Similarly, Fig. 4 compares the E-field for the two different widths of the CPW, along a cross section at 250 μm below the PCB top surface [Fig. 4(a)] and directly under the CPW resonator [Fig. 4(b)]. In this particular arrangement, the E-field close to the resonator increases 2.5 times when the center conductor is widened [Fig. 4(b)], whilst the difference is less marked deeper in the PCB [Fig. 4(a)].

D. Contact Pad Tapering

Despite maintaining a characteristic impedance of 50 Ω, the abruptly tapered contact pads [such as that depicted in Fig. 1(c)] can generate a shift in the resonance to lower frequencies and an additional peak [7], since the resonator is sensitive to geometric changes close to the boundaries as the evanescent EM wave decays over this length-scale. The simulation in Fig. 2(e) depicts higher E-fields extending further from the central conductor when the contact pads on the PCB and the sample chip are larger and more sharply tapered. Note that power is coupled to the ground planes at the PCB-chip transition and coplanar waveguide tapering, irrespective of impedance matching.

IV. Transmission Measurements at Millikelvin

We now present low-power microwave transmission measurements of Nb CPW resonators at milli-Kelvin temperatures, comparing the effect of parasitic modes on the Q-factor and

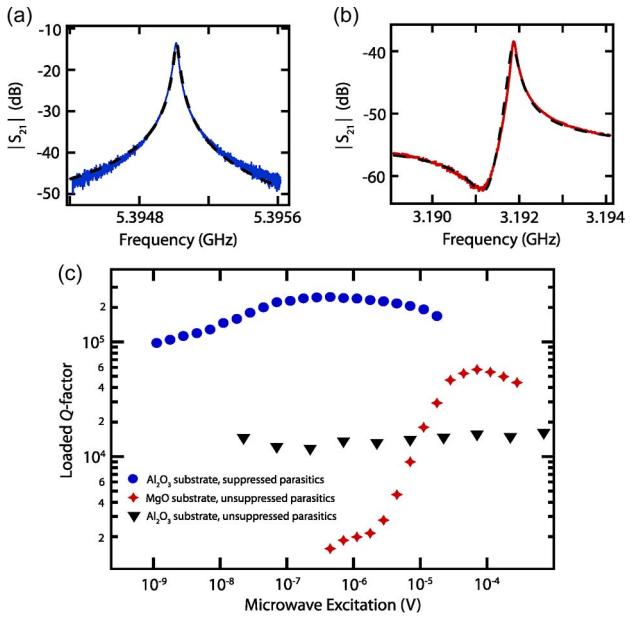

Fig. 5. S_{21} spectra for Nb resonator on (a) sapphire (blue) and (b) MgO (red) at 10 mK and −100 dB excitation power. Black lines are fits to equation (2) in [9] from which Q-factors were extracted. (c) Loaded Q-factors for Nb resonators on sapphire (blue, black) and MgO (red) substrates versus microwave voltage at 10 mK.

resonance line-shape. Data was taken on both sapphire (Al_2O_3) and MgO substrates to compare dielectric loss at low powers and temperatures, as shown in Fig. 5. In the case where parasitic fields are mitigated, as described above, the line-shapes appear more Lorentzian [Fig. 5(a)], since coherent interference between direct and parallel paths is suppressed. In contrast, the presence of parallel signal paths leads to a strongly asymmetric resonator response [Fig. 5(b)]. Asymmetric line-shapes in superconducting resonators have been noted previously [8]–[13] and described using a corresponding equivalent circuit model [4] or an additional complex background term to account for radiation coupling via a parallel path [9].

Using the model in [9] we extract the loaded Q-factor using a least squares fit to the resonator frequency response. Fig. 5(c) shows the loaded Q-factors for three different setups, each with varying degrees of parasitic coupling. Two types of loss mechanism are apparent. In the case of the MgO, the presence of many two-level charge traps in either the dielectric or the interface between the superconductor and the dielectric substrate strongly limit the Q-factor at low excitation. For the sapphire devices, such dependence at low excitation is more difficult to observe, since the loss from two-level defects is slight. Only when parasitic pathways have been mitigated using the means described here is it possible to observe the slight decrease in the loaded-Q originating from two-level defects [4], [5].

V. Conclusion

Results from experiment and simulation suggest there is no single dominant mechanism that accounts for parasitic losses in Nb resonators. Here we have reported several strategies to reduce the strength of the parasitic interference. These include a high density of vias in the PCB, spaced at $\lambda/20$ or less, to improve the grounding. Ideally, a solid via "fence" along both sides of the CPW, would further reduce the extent to which the field permeates the dielectric. Tightly spaced wire-bonds (< 0.3 mm) around the resonator chip, grounding it to the PCB are also important. Minimizing the SMA launcher diameter and matching it to the width of the PCB track, whilst maintaining 50 Ω characteristic impedance, helps to reduce the power coupled to the ground plane. As shown previously [14] the existence of the parallel path coincides with an asymmetric line-shape. Since this path is not lossless, power from the resonator is dissipated and the loaded Q-factor is reduced. Further care is required at transitions in the geometry such as abruptly tapered contact pads.

References

[1] P. K. Day, H. G. LeDuc, B. A. Mazin, A. Vayonakis, and J. Zmuidzinas, "A broadband superconducting detector suitable for use in large arrays," *Nature*, vol. 425, no. 6960, pp. 817–821, Oct. 2003.

[2] I. Siddiqi, R. Vijay, F. Pierre, C. M. Wilson, M. Metcalfe, C. Rigetti, L. Frunzio, and M. H. Devoret, "RF-driven Josephson bifurcation amplifier for quantum measurement," *Phys. Rev. Lett.*, vol. 93, no. 20, pp. 207002-1–207002-4, Nov. 2004.

[3] A. Wallraff, D. I. Schuster, A. Blais, L. Frunzio, R.-S. Huang, J. Majer, S. Kumar, S. M. Girvin, and R. J. Schoelkopf, "Strong coupling of a single photon to a superconducting qubit using circuit quantum electrodynamics," *Nature*, vol. 431, no. 7005, pp. 162–167, Sep. 2004.

[4] A. D. O'Connell, M. Ansmann, R. C. Bialczak, M. Hofheinz, N. Katz, C. Erik Lucero, M. McKenney, H. Neeley, E. M. Wang, A. N. Weig, and J. M. Cleland, "Microwave dielectric loss at single photon energies and millikelvin temperatures," *Appl. Phys. Lett.*, vol. 92, no. 11, pp. 112903-1–112903-3, Mar. 2008.

[5] P. Macha, S. H. W. van der Ploeg, G. Oelsner, E. Il'ichev, H.-G. Meyer, S. Wünsch, and M. Siegel, "Losses in coplanar waveguide resonators at millikelvin temperatures," *Appl. Phys. Lett.*, vol. 96, no. 6, pp. 062503-1–062503-3, Feb. 2010.

[6] M. Goppl, A. Fragner, M. Baur, R. Bianchetti, S. Filipp, J. M. Fink, P. J. Leek, G. Puebla, L. Steffen, and A. Wallraff, "Coplanar waveguide resonators for circuit quantum electrodynamics," *J. Appl. Phys.*, vol. 104, no. 11, pp. 113904-1–113904-8, Dec. 2008.

[7] J. M. Hornibrook, E. E. Mitchell, C. J. Lewis, and D. J. Reilly, "Parasitic losses in Nb superconducting resonators," *Phys. Proc.*, vol. 36, pp. 187–192, 2012.

[8] H. Paik, D. I. Schuster, L. S. Bishop, G. Kirchmair, G. Catelani, A. P. Sears, B. R. Johnson, M. J. Reagor, L. Frunzio, L. I. Glazman, S. M. Girvin, M. H. Devoret, and R. J. Schoelkopf, "Observation of high coherence in Josephson junction qubits measured in a three-dimensional circuit QED architecture," *Phys. Rev. Lett.*, vol. 107, no. 24, pp. 240501-1–240501-5, Dec. 2011.

[9] J. M. Sage, V. Bolkhovsky, W. D. Oliver, B. Turek, and P. B. Welander, "Study of loss in superconducting coplanar waveguide resonators," *J. Appl. Phys.*, vol. 109, no. 6, pp. 063915-1–063915-10, Mar. 2011.

[10] A. E. Miroshnichenko, S. Flach, and Y. S. Kivshar, "Fano resonances in nanoscale structures," *Rev. Mod. Phys.*, vol. 82, no. 3, pp. 2257–2298, Aug. 2010.

[11] A. Megrant, C. Neill, R. Barends, B. Chiaro, Y. Chen, L. Feigl, J. Kelly, E. A. Lucero, M. Mariantoni, P. J. J. OMalley, D. Sank, A. Vainsencher, J. Wenner, T. C. White, Y. Yin, J. Zhao, C. J. Palmstrm, J. M. Martinis, and A. N. Cleland, "Planar superconducting resonators with internal quality factors above one million," *Appl. Phys. Lett.*, vol. 100, no. 11, pp. 113510-1–113510-4, Mar. 2012.

[12] M. Khalil, M. J A Stoutimore, F. C. Wellstood, and K. D. Osborn, "An analysis method for asymmetric resonator transmission applied to superconducting devices," *J. Appl. Phys.*, vol. 111, no. 5, pp. 054510-1–054510-6, Mar. 2012.

[13] K. Geerlings, S. Shankar, E. Edwards, L. Frunzio, R. J. Schoelkopf, and M. H. Devoret, "Improving the quality factor of microwave compact resonators by optimizing their geometrical parameters," *Appl. Phys. Lett.*, vol. 100, no. 19, pp. 192601-1–192601-3, May 2012.

[14] J. M. Hornibrook, E. E. Mitchell, and D. J. Reilly, arXiv: /0440043 cond-mat.supr-con.